

Shear viscosity to entropy density ratio in nuclear multifragmentation

Subrata Pal

Department of Nuclear and Atomic Physics, Tata Institute of Fundamental Research, Homi Bhabha Road, Mumbai 400005, India

(Received 12 April 2010; published 17 May 2010)

Nuclear multifragmentation in intermediate-energy heavy-ion collisions has long been associated with liquid-gas phase transition. We calculate the shear viscosity to entropy density ratio η/s for an equilibrated system of nucleons and fragments produced in multifragmentation within an extended statistical multifragmentation model. The temperature dependence of η/s exhibits behavior surprisingly similar to that of H_2O . In the coexistence phase of fragments and light particles, the ratio η/s reaches a minimum of depth comparable to that for water in the vicinity of the critical temperature for liquid-gas phase transition. The effects of freeze-out volume and surface symmetry energy on η/s in multifragmentation are studied.

DOI: [10.1103/PhysRevC.81.051601](https://doi.org/10.1103/PhysRevC.81.051601)

PACS number(s): 25.70.Pq, 24.60.-k, 25.70.Mn

Understanding the behavior of nuclear matter under extreme conditions has been one of the most important challenges in heavy-ion physics. Multifragmentation in intermediate-energy heavy-ion collisions provides a key mechanism to address this issue; it occurs when an excited nucleus expands and breaks up into various fragments and light particles [1–3]. The final yield distribution is quite sensitive to the internal excitation, breakup density of the nucleus, and the symmetry energy part of the binding energy of the fragments [4–8].

Due to van der Waals nature of the nucleon-nucleon interaction, it is expected that multifragmentation may exhibit features of liquid-gas phase transition [1,2]. Evidence of this is provided by the observation of the nuclear caloric curve relating excitation energy to the temperature of the breakup source [9–11]. Extensive studies have been carried out to understand the dependence of the caloric curve on the system size and particularly on the density dependence of nuclear symmetry energy, which is poorly constrained [12].

However, multifragmentation studies are mostly confined to the effects of the state variables on the thermodynamic properties of the system, whereas transport properties of the dynamically evolving system of nucleons and fragments formed in fragmentation have received little attention. Since the transport coefficients characterize the dynamics of fluctuation of the dissipative fluxes in a medium [13], their knowledge is essential for a better understanding of the fragmentation observables. Recently, considerable attention has been focused primarily on the shear viscosity coefficient that involves the transport of momentum due to the velocity gradient in an anisotropic medium. Empirical observation [14] of the temperature dependence of the shear viscosity to entropy density ratio η/s for water (as well as for He and Ne_2) reveals a minimum in the vicinity of the critical temperature T_c for liquid-gas phase transition. Furthermore, a lower bound of $\eta/s \geq 1/4\pi$, obtained by Kovtun-Son-Starinets (KSS) [15] in certain gauge theories, has been speculated [15] to be valid for several substances in nature.

In heavy-ion collisions at energy $E_{\text{lab}} \lesssim 1000$ MeV/nucleon, the shear viscosity coefficient has been estimated for nucleon transport in the Uhlenbeck-Uehling equations [16]. Analysis of the observed transverse flow of nucleons in the

microscopic Quantum Molecular Dynamics (QMD) model in Au + Au, Nb + Nb, and Ca + Ca central collisions at energy $E_{\text{lab}} = 400\text{--}1200$ MeV/nucleons requires shear viscosity of $30 < \eta < 60$ MeV/($\text{fm}^2 \text{c}$) [17]. Since the degrees of freedom in these studies involve only nucleons, the η estimate is relevant only in the early stages of the reaction. Fragments formed due to correlations and fluctuations of the system that go beyond the mean field dynamics of nucleon transport should result in a different shear viscosity. At freeze-out, the momentum transport and thereby the shear viscosity is mostly effected by long-range Coulomb interaction between the charged particles.

In this article, we estimate the shear viscosity to entropy density ratio η/s of an equilibrated system of fragments and/or light particles produced from multifragmentation within a modified microcanonical statistical multifragmentation model (SMM) [2] that has successfully reproduced several observables [2–4,18]. We show that η/s decreases as a function of temperature of the system, exhibits a minimum at the coexisting liquid-gas phase composed of intermediate-mass fragments and light particles, and increases again at high temperature in a system of light particles. The estimated minimum of η/s is comparable to that for water in the vicinity of a critical point for liquid-gas phase transition.

In the SMM, a hot source with mass and charge (A_0, Z_0) at temperature T expands to a freeze-out volume $V = (1 + \chi)V_0$ and undergoes prompt statistical breakup; here V_0 is the normal nuclear volume and $\chi \geq 0$ is input parameter. We start with the grand-canonical version of SMM, which consists of minimizing the free energy F of the system

$$F(T) = \sum_{A,Z} N_{A,Z} [f_{A,Z}^{\text{tr}} + f_{A,Z}^*] + F_c, \quad (1)$$

under conservation of mass $A_0 = \sum_{A,Z} N_{A,Z} A$ and charge $Z_0 = \sum_{A,Z} N_{A,Z} Z$. The translational energy of a nuclear species with mass and charge (A, Z) is

$$f_{A,Z}^{\text{tr}} = -T \left[\log \left(\frac{g_{A,Z} V_f A^{3/2}}{\lambda_T^3} \right) - \frac{\log(N_{A,Z}!)}{N_{A,Z}} \right], \quad (2)$$

where the thermal wavelength is $\lambda_T = \sqrt{2\pi\hbar^2/mT}$ and m is the nucleon mass. The spin degeneracy is denoted by $g_{A,Z}$, and the free volume is $V_f = V - V_0$. The multiplicity $N_{A,Z}$

of the fragment (A, Z) is then given by [2,8]

$$N_{A,Z} = \frac{g_{A,Z} V_f A^{3/2}}{\lambda_T^3} \exp \left\{ - \left[f_{A,Z}^* - \mu_B A - \mu_Q Z + \frac{2C_c Z Z_0}{(1+\chi)^{1/3} A_0^{1/3}} - \frac{C_c A Z_0^2}{3(1+\chi)^{1/3} A_0^{4/3}} \right] / T \right\}. \quad (3)$$

The baryon and charge chemical potentials μ_B and μ_Q are obtained from mass and charge conservation. The internal free energy of the species (A, Z) is

$$f_{A,Z}^* = -B_{A,Z} - \frac{T^2}{\epsilon_0} A + \beta_0 A^{2/3} \left[\left(\frac{T_c^2 - T^2}{T_c^2 + T^2} \right)^{5/4} - 1 \right] - \frac{C_c Z^2}{(1+\chi)^{1/3} A^{1/3}}, \quad (4)$$

where the parameters are $\epsilon_0 = 16$ MeV, $\beta_0 = 18$ MeV, and $T_c = 18$ MeV. The fragments here are assumed to be at normal density. The Coulomb repulsion between the fragment F_c in Eq. (1) is evaluated in the Wigner-Seitz approximation and corresponds to the last term in Eq. (4). The Coulomb self-energy of a fragment is included in its binding energy $B_{A,Z}$. The last two terms in Eq. (3) stem from homogeneous term of the Wigner-Seitz approximation [2,8]. Light nuclei with $A < 5$ are considered point particles with no internal degrees of freedom, so that the bulk and surface contributions to internal free energy $f_{A,Z}^*$ [second and third terms of Eq. (4), respectively] are neglected, except for α particle, where the bulk contribution is retained as usual [2]. For these light nuclei, experimental values for binding energy are used. For heavier nuclei $A \geq 5$, the spin degeneracy $g_{A,Z} = 1$, and for binding energy $B_{A,Z}$, the computed liquid drop mass (LDM) formula of Ref. [8] is used:

$$B_{A,Z} = C_v A - C_s A^{2/3} - C_c \frac{Z^2}{A^{1/3}} + C_d \frac{Z^2}{A}, \quad (5)$$

where $C_i = a_i [1 - k_i (A - 2Z)^2 / A^2]$ and $i = v, s$ correspond to the volume and surface terms, respectively. The volume and surface contributions to symmetry energy give $E_{\text{sym}} = C_{\text{sym}} (A - 2Z)^2 / A^2$, where $C_{\text{sym}} = a_v k_v - a_s k_s / A^{1/3}$. Two versions of the LDM formula are used here, dubbed as LDM1 and LDM2 [8], to study surface symmetry energy effects on the η/s ratio. The simpler LDM1 has $k_s = 0$ (also $C_d = 0$) and thus neglects the surface corrections to the symmetry energy. The complete LDM2 formula preserves all the terms.

The energy conservation of the fragmenting source leads to

$$E_{\text{sour}}^{\text{gs}} + E^* = E^{\text{tr}}(T) + \sum_{A,Z} N_{A,Z} [-B_{A,Z} + \epsilon_{A,Z}^*] + \frac{C_c}{(1+\chi)^{1/3}} \frac{Z_0^2}{A_0^{1/3}} - \frac{C_c}{(1+\chi)^{1/3}} \times \sum_{A,Z} N_{A,Z} \frac{Z^2}{A^{1/3}}, \quad (6)$$

where $E_{\text{sour}}^{\text{gs}}$ is the ground-state energy of the source and $\epsilon_{A,Z}^*(T)$ denotes the excitation energy of the fragment (A, Z)

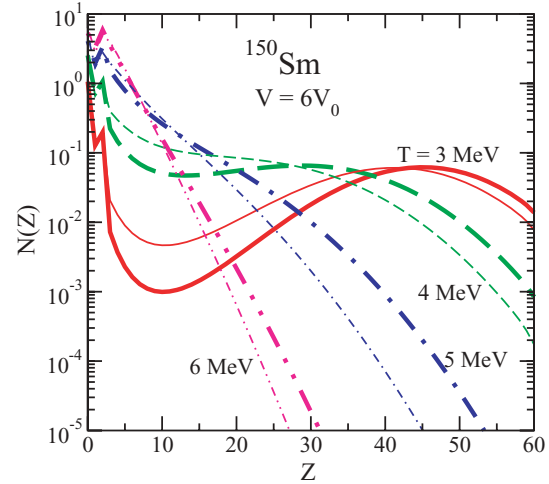


FIG. 1. (Color online) Charge distribution in the breakup of the ^{150}Sm nucleus at various temperatures T at a freeze-out volume of $V = 6V_0$ in the LDM1 (thin lines) and LDM2 (thick lines) mass formulas.

at temperature T with a translational energy $\epsilon_{A,Z}^{\text{tr}} = 3T/2$. Equation (6) allows us to extract the excitation energy E^* of the source at a given T and thereby construct the nuclear caloric curve.

In the grand-canonical SMM, the probability distribution of the fragment yield, $P_{A,Z} = N_{A,Z} / \sum_{A,Z} N_{A,Z}$, allows one to generate [19] a Monte Carlo microcanonical ensemble of fragments with exact conservations of mass A_0 , charge Z_0 and total energy of the source. The fragments in a microcanonical ensemble are placed in a nonoverlapping fashion within a spherical freeze-out volume V . These particles are then allowed to evolve in time under Coulomb repulsion within the freeze-out volume with periodic boundary conditions in the configuration space. Finally, collision between the fragments enforce kinetic equilibration when the system is found to approach momentum isotropization [20]. The shear viscosity of this dynamically evolving equilibrated system is then estimated.

In Fig. 1, we show the charge distribution for the breakup of ^{150}Sm at $T = 3, 4, 6$ MeV in the LDM1 and LDM2 mass formulas. At low temperature, $T = 3$ MeV, the system is characterized by few light particles and a massive nucleus (liquid phase) close to the source charge. The minimum of the free energy $F = E - TS$ is essentially controlled by the surface term in Eq. (4) that favors one massive nucleus instead of small fragments with a larger total surface. With increasing temperature, more intermediate-mass fragments (IMFs; $3 \leq Z \leq 15$) are produced. Here, the $-TS$ term in free energy, dominated by binding energy and Coulomb repulsion, favors the breakup into small fragments [3]. Eventually at large T , only light particles are produced (gas phase). Compared to the LDM1 set, the inclusion of surface symmetry energy in LDM2 that is important for light nuclei of mass $A < 25$ [8] leads to the suppression of isospin symmetric IMFs and an enhancement of neutron-rich heavier nuclei.

In order to gain insight into the quantitative effects from the two mass formulas, we show the multiplicity of different species as a function of temperature in Fig. 2. At $T < 3$ MeV,

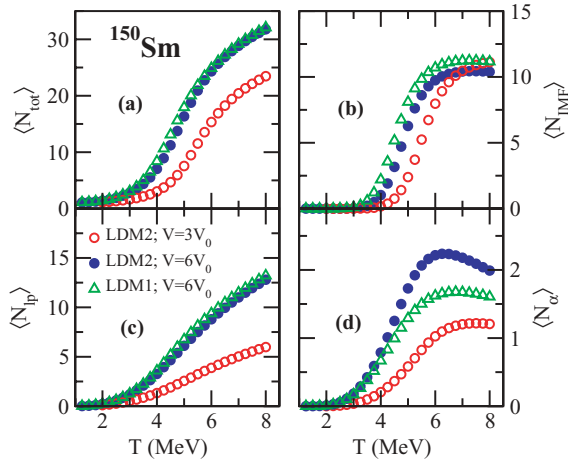


FIG. 2. (Color online) Temperature dependence of multiplicity of (a) all particles, N_{tot} , (b) IMFs, N_{IMF} , (c) light particles with $A < 5$ except α , N_{lp} , and (d) α , N_{α} , in the breakup of the ^{150}Sm nucleus in LDM1 (triangles) and LDM2 (solid circles) mass formulas at a freeze-out volume of $V = 6V_0$ and in LDM2 (open circles) at $V = 3V_0$.

where the yield is dominated by a massive fragment, the symmetry energy effects are imperceptible in the LDM1 (triangles) and LDM2 (solid circles) sets at the same freeze-out volume $V = 6V_0$. At moderate and high temperatures, the total multiplicity N_{tot} in the LDM2 set is reduced as surface symmetry energy favors heavier nuclei with large neutron-proton asymmetry. This leads to a reduction in the yields of more isospin symmetric IMFs, N_{IMF} , and light nuclei, N_{lp} , in comparison to the LDM1 set. Also shown in Fig. 2, the particle abundances in the LDM2 set at a smaller freeze-out volume $V = 3V_0$, where, as expected, the yields are reduced.

The nuclear caloric curve [2,9–11] associated with the fragmentation of ^{150}Sm nucleus is shown in Fig. 3. At $3 \lesssim E^*/A \lesssim 8$ MeV, the caloric curve exhibits a slow but monotonous increase of temperature with excitation energy [10,21,22], which may be a signature of liquid-gas phase transition. This behavior stems from the energy-conservation

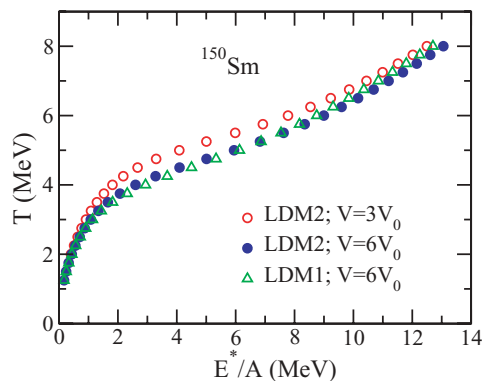


FIG. 3. (Color online) Caloric curve expressing excitation energy per nucleon E^*/A vs temperature T for the breakup of the ^{150}Sm nucleus in LDM1 (triangles) and LDM2 (solid circles) mass formulas at a freeze-out volume of $V = 6V_0$ and in LDM2 (open circles) at $V = 3V_0$.

constraint of Eq. (6), when an appreciable amount of energy is used to produce abundant IMFs and light particles. The experimentally observed plateau [10,11] in the caloric curve may result if the breakup occurs at a fixed pressure (i.e., multifragmentation is an isobaric process) [21,23,24], in contrast to the fixed freeze-out volume employed here, or if the fragments are expanded [25], unlike the fragments here assumed to be at normal nuclear density. Note that in this excitation range, the massive fragments with large binding and internal excitation in the LDM2 set (solid circles) lead to slightly higher temperatures (or conversely smaller E^*/A) compared to the LDM1 set (triangles). At $E^*/A > 8$ MeV, the smaller multiplicity of light particles, which have no internal degrees of freedom, in the LDM2 set results in lower temperatures relative to the LDM1 set. At freeze-out volume $V = 3V_0$ in LDM2, the breakup temperature is consistently higher, as more massive and fewer fragments are produced.

The entropy $S = -dF/dT$ in the microcanonical ensemble of fragments is determined using the conventional thermodynamic relation [2,3]

$$S = \log \prod_{A,Z} (2g_{A,Z} + 1) + \log \prod_{A,Z} A^{3/2} - \ln A_0^{3/2} - \log \left(\prod_{A,Z} (N_{A,Z}!) \right) + (M - 1) \log (V_f / \lambda_T^3) + 1.5(M - 1) - \sum_{A,Z} \partial f_{A,Z}^* / \partial T, \quad (7)$$

where the total multiplicity in an event is $M = \sum_{A,Z} N_{A,Z}$ and the last term corresponds to entropy contribution from the bulk and surface terms in the internal free energy of Eq. (4).

In Fig. 4(a), the entropy per nucleon S/A is shown as a function of temperature for the fragmentation of ^{150}Sm . In the temperature range $4 \leq T \leq 6$ MeV, associated with the liquid-gas mixed phase in the caloric curve, the entropy shows a rapid increase with temperature. In this region, abundant

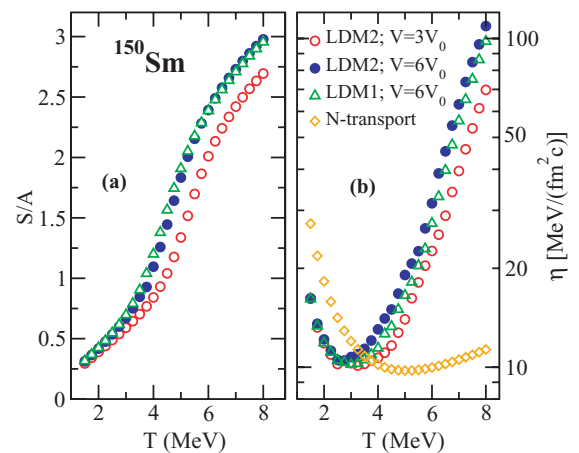


FIG. 4. (Color online) (a) Entropy per nucleon S/A and (b) shear viscosity coefficient η as a function of temperature for the breakup of the ^{150}Sm nucleus in LDM1 (triangles) and LDM2 (solid circles) mass formulas at a freeze-out volume of $V = 6V_0$ and in LDM2 (open circles) at $V = 3V_0$. Shear viscosity in nucleon transport calculation [16] is shown by the diamonds.

IMFs are produced in the LDM1 set (triangles) with smaller internal degrees of freedom that leads to somewhat higher entropy than in the LDM2 set (solid circles) with more massive fragments. At $V = 3V_0$ in LDM2, suppression of particle yield leads to a reduction in entropy.

For time-evolving system of fragments in equilibrium, the shear viscosity due to momentum transport (via Coulomb scattering between the fragments) can be computed from the Kubo relation [20,26] or the classical kinetic theory [27]. The Kubo formula employs the linear-response theory to relate the transport coefficients as correlations of dissipative fluxes. However, it provides the total viscosity of the system, not from individual species. On the other hand, in the kinetic theory, the total shear viscosity of a multicomponent system can be expressed as the sum from individual contribution as $\eta \simeq (1/3) \sum_i n_i \langle p_i \rangle \lambda_i$, where n_i is the number density, $\langle p_i \rangle$ is the average momentum, and λ_i is the mean free path of the i th species. Moreover, $\lambda_i = 1/\sum_j n_j \sigma_{ij}$, where σ_{ij} is the collisional cross section which is taken as that for the usual Coulomb scattering. The average thermal momentum of the particle in the nonrelativistic limit is $\langle p_i \rangle = m_i \langle v_i \rangle = \sqrt{8m_i T/\pi}$. The results presented here are in the kinetic theory limit; we have checked the total η and obtained matches with that from the Kubo formalism.

In Fig. 4(b), we present the shear viscosity η for an equilibrated ensemble from fragmentation of ^{150}Sm . At temperatures $T < 3$ MeV (corresponding to the liquid phase), the shear viscosity is found to rapidly increase with decreasing T . For the dilute system comprising a large nucleus and a few light particles, the mean free path λ is large. Thus, a fragment can transport momentum over a large distance, resulting in large η . At intermediate $T \sim 3\text{--}6$ MeV (corresponding to the coexistence region), the magnitude of viscosity is determined by competing effects between the size and multiplicity of the fragments in the system. The Coulomb repulsion forces the two colliding nuclei to occupy the available free space (void), which in turn will collide with the neighboring nucleus and so on. This procedure can effectively transport momentum over a large distance and produce a large viscosity [14]; the coefficient grows with temperature as $\eta \sim T^{1/2}$. In general, the viscosity $\eta_{A,Z}$ of a species (A, Z) was found to progressively increase from heavier to lighter particles that have larger Z/A ratios. Compared to LDM1 at $V = 6V_0$, the heavier fragments in LDM2 in the liquid-gas mixed phase and somewhat higher temperature (see also Figs. 2 and 3) are more effective for momentum transport, resulting in an increased η . This is due to $\eta_{A,Z}$ values being $\sim 30\%$ higher in the LDM2 than in the LDM1 formula at a given T . At a smaller freeze-out volume $V = 3V_0$, fewer fragment collisions as well as smaller density of voids inhibit momentum transport and thereby reduce dissipation in the medium.

For orientation, we also show in Fig. 4(b) the shear viscosity from analytical fit to the numerical evaluation of η , obtained by Danielewicz [16], in the Uhlenbeck-Uehling transport equations within a first-order Chapman-Enskog approximation:

$$\eta = (1700/T^2)(n/n_0)^2 + [22/(1 + 10^{-3}T^2)](n/n_0)^{0.7} + 5.8T^{1/2}/(1 + 160T^2). \quad (8)$$

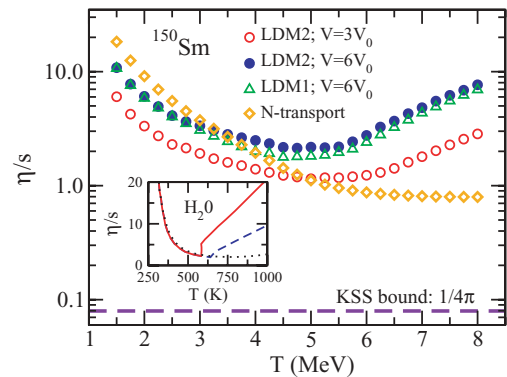


FIG. 5. (Color online) Shear viscosity to entropy density ratio η/s as a function of temperature T for the breakup of ^{150}Sm nucleus in LDM1 (triangles) and LDM2 (solid circles) mass formulas at a freeze-out volume of $V = 6V_0$ and in LDM2 (open circles) at $V = 3V_0$. The η/s from nucleon transport is shown by the diamonds. The inset shows η/s vs T for water from Ref. [14] for an isobar at the critical pressure, $P_c = 22.6$ MPa (dashed lines), one below it at $P = 10$ MPa (solid line), and the other above it at $P = 100$ MPa (dotted line).

In this microscopic calculation, where the relevant degrees of freedom are nucleons in the colliding nucleus, significant momentum transport by the nucleons in the early stages of reactions (not considered in our study) leads to faster growth in viscosity at small $T \sim 1\text{--}2$ MeV. In contrast, at $T \gtrsim 4$ MeV, the present study clearly underscores the importance of finite-sized fragments from multifragmentation (missing in the transport calculations [16]) that substantially enhance the viscosity in the medium.

Figure 5 shows the shear viscosity to entropy density ratio η/s as a function of temperature in multifragmentation of ^{150}Sm . The η/s value gradually decreases as a function of rising temperature up to $T \sim 4$ MeV in the liquid phase (system dominated by a massive nucleus) and then increases again at $T \gtrsim 6$ MeV in the gas phase (system of light particles). At $T \approx 5$ MeV, that is, close to the critical temperature for multifragmentation (liquid-gas coexistence phase) [1–4,9], the η/s reaches a minimum. In the LDM2 mass formula at a freeze-out of $V = 6V_0$, a minimum of $(\eta/s)_{\min} \approx 2.1$ is obtained. In the absence of surface symmetry energy in LDM1, the $(\eta/s)_{\min}$ turns to be somewhat smaller. While at a smaller freeze-out volume of $V = 3V_0$, the η/s magnitude is even smaller. However, the $(\eta/s)_{\min}$ estimated in multifragmentation is significantly above the conjectured KSS lower bound of $1/4\pi$ [15]. If we adopt the entropy of the LDM2 set with $V = 6V_0$ and η of Eq. (8) for nucleon transport [16], then η/s is seen (Fig. 5) to decrease continuously with increasing T .

Interestingly, the $(\eta/s)_{\min}$ obtained in multifragmentation is comparable to the minimum value for isobars passing in the vicinity of the critical temperature T_c for liquid-gas phase transition in water [14]. For H_2O , when an isobar passes through the critical point (shown in the inset of Fig. 5), the $(\eta/s)_{\min}$ forms a cusp at T_c . When the isobar passes below P_c , the minimum is at $T < T_c$ with a discontinuous change across the phase transition. For an isobar passing above P_c ,

a broad minimum is found at a T slightly above T_c . In fact, the smallest value of η/s corresponds to the most difficult condition for the transport of momentum. In analogy to this observation, if multifragmentation is at a fixed freeze-out volume, the hot system samples a range of η/s corresponding to different values of pressures at different temperatures. If the breakup volume varies, the different values of η/s found at $V/V_0 = 3$ and 6 in Fig. 5 imply that the system samples a large range of η/s in the (P, V) plane to give an average. On the other hand, if freeze-out is reached at a fixed pressure [23,24] (and close to P_c), this would result in a rapid increase in η/s at $|T - T_c| > 0$ comparable to the rise observed for H_2O [14].

In summary, we have studied the thermodynamic and transport properties in fragmentation of a nucleus within a statistical multifragmentation model. For the equilibrated system of fragments and light particles evolving under Coulomb repulsion, we find the shear viscosity to entropy density ratio η/s exhibits a minimum at a temperature of $T \approx 5$ MeV in the coexistence phase of intermediate-mass fragments and light particles. The minimum value of $(\eta/s)_{\min} \simeq 2$ in multifragmentation is comparable to that at the critical point for liquid-gas phase transition in H_2O . The temperature dependence of η/s is somewhat sensitive to the surface effects on symmetry energy and depends rather strongly on the freeze-out volume.

-
- [1] D. H. E. Gross, *Rep. Prog. Phys.* **53**, 605 (1990).
 [2] J. P. Bondorf, A. S. Botvina, A. S. Iljinov, I. N. Mishustin, and K. Sneppen, *Phys. Rep.* **257**, 133 (1995).
 [3] C. B. Das, S. Das Gupta, W. G. Lynch, A. Z. Mekjian, and M. B. Tsang, *Phys. Rep.* **406**, 1 (2005).
 [4] A. S. Botvina, O. V. Lozhkin, and W. Trautmann, *Phys. Rev. C* **65**, 044610 (2002).
 [5] A. Le Fèvre *et al.*, *Phys. Rev. Lett.* **94**, 162701 (2005).
 [6] D. V. Shetty, S. J. Yennello, and G. A. Souliotis, *Phys. Rev. C* **76**, 024606 (2007).
 [7] M. B. Tsang *et al.*, *Phys. Rev. Lett.* **92**, 062701 (2004).
 [8] S. R. Souza, M. B. Tsang, R. Donangelo, W. G. Lynch, and A. W. Steiner, *Phys. Rev. C* **78**, 014605 (2008).
 [9] J. Pochodzalla *et al.*, *Phys. Rev. Lett.* **75**, 1040 (1995).
 [10] J. B. Natowitz *et al.*, *Phys. Rev. C* **65**, 034618 (2002).
 [11] M. D'Agostino *et al.*, *Nucl. Phys. A* **699**, 795 (2002).
 [12] P. Danielewicz, R. Lacey, and W. G. Lynch, *Science* **298**, 1592 (2002).
 [13] L. D. Landau and E. M. Lifshitz, *Fluid Mechanics* (Pergamon Press, New York, 1987), Vol. 6.
 [14] L. P. Csernai, J. I. Kapusta, and L. D. McLerran, *Phys. Rev. Lett.* **97**, 152303 (2006).
 [15] G. Policastro, D. T. Son, and A. O. Starinets, *Phys. Rev. Lett.* **87**, 081601 (2001); P. K. Kovtun, D. T. Son, and A. O. Starinets, *ibid.* **94**, 111601 (2005).
 [16] P. Danielewicz, *Phys. Lett. B* **146**, 168 (1984).
 [17] B. Schürmann, *Mod. Phys. Lett. A* **3**, 1137 (1988).
 [18] S. R. Souza, R. Donangelo, W. G. Lynch, and M. B. Tsang, *Phys. Rev. C* **76**, 024614 (2007).
 [19] S. Pal, S. K. Samaddar, A. Das, and J. N. De, *Nucl. Phys. A* **586**, 466 (1995).
 [20] S. Pal, *Phys. Lett. B* **684**, 211 (2010).
 [21] C. E. Aguiar, R. Donangelo, and S. R. Souza, *Phys. Rev. C* **73**, 024613 (2006).
 [22] A. Botvina, G. Chaudhuri, S. Das Gupta, and I. Mishustin, *Phys. Lett. B* **668**, 414 (2008).
 [23] J. B. Elliott and A. S. Hirsch, *Phys. Rev. C* **61**, 054605 (2000).
 [24] P. Chomaz, V. Duflot, and F. Gulminelli, *Phys. Rev. Lett.* **85**, 3587 (2000).
 [25] S. R. Souza *et al.*, *Phys. Rev. C* **80**, 041602(R) (2009).
 [26] R. Kubo, *Rep. Prog. Phys.* **29**, 255 (1966).
 [27] F. Reif, *Fundamentals of Statistical and Thermal Physics* (McGraw-Hill, Singapore, 1965).